JACS
JOURNAL OF THE AMERICAN CHEMICAL SOCIETY
Article
pubs.acs.org/JACS

Polymorphic Copper Iodide Clusters: Insights into the Mechanochromic Luminescence Properties

Quentin Benito,[†] Xavier F. Le Goff,[‡] Sébastien Maron,[†] Alexandre Fargues,[§] Alain Garcia,[§] Charlotte Martineau,[∥] Francis Taulelle,[∥] Samia Kahlal,[⊥,#] Thierry Gacoin,[†] Jean-Pierre Boilot,[†] and Sandrine Perruchas*[,†]

[†]Laboratoire de Physique de la Matière Condensée (PMC), CNRS - Ecole Polytechnique, 91128 Palaiseau Cedex, France

[‡]Laboratoire Hétéroéléments et Coordination (DCPH), CNRS - Ecole Polytechnique, 91128 Palaiseau Cedex, France

[§]Institut de Chimie de la Matière Condensée de Bordeaux (ICMCB) - CNRS, 87 Avenue du Docteur A. Schweitzer, 33608 Pessac Cedex, France

[∥]Tectospin, Institut Lavoisier de Versailles (ILV), UMR CNRS 8180, Université de Versailles St-Quentin en Yvelines (UVSQ), 45, avenue des Etats-Unis, 78035 Versailles Cedex, France

[⊥]Institut des Sciences Chimiques de Rennes (ISCR), UMR CNRS 6226, Université de Rennes 1, 35042 Rennes Cedex, France

[#]Université Européenne de Bretagne, 5 bd. Laënnec, 35000 Rennes, France

Supporting Information

ABSTRACT: An in-depth study of mechanochromic and thermochromic luminescent copper iodide clusters exhibiting structural polymorphism is reported and gives new insights into the origin of the mechanochromic luminescence properties. The two different crystalline polymorphs exhibit distinct luminescence properties with one being green emissive and the other one being yellow emissive. Upon mechanical grinding, only one of the polymorphs exhibits great modification of its emission from green to yellow. Interestingly, the photophysical properties of the resulting partially amorphous crushed compound are closed to those of the other yellow polymorph. Comparative structural and optical analyses of the different phases including a solution of clusters permit us to establish a correlation between the Cu−Cu bond distances and the luminescence properties. In addition, the local structure of the $[Cu_4I_4P_4]$ cluster cores has been probed by ^{31}P and ^{65}Cu solid-state NMR analysis, which readily indicates that the grinding process modifies the phosphorus and copper atoms environments. The mechanochromic phenomenon is thus explained by the disruption of the crystal packing within intermolecular interactions inducing shortening of the Cu−Cu bond distances in the $[Cu_4I_4]$ cluster core and eventually modification of the emissive state. These results definitely establish the role of cuprophilic interactions in the mechanochromism of copper iodide clusters. More generally, this study constitutes a step further into the understanding of the mechanism involved in the mechanochromic luminescent properties of metal-based compounds.

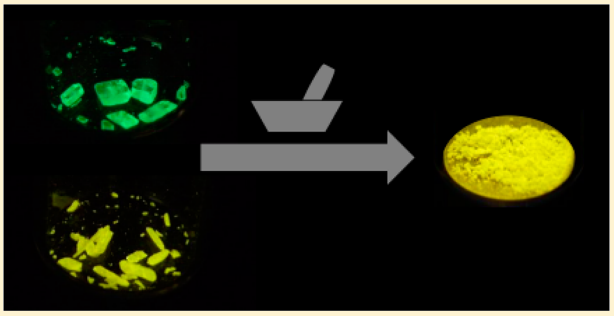

INTRODUCTION

Research on stimuli-responsive luminescent materials have gained considerable interest for the development of smart photoactive materials for various technological applications.[1−3] In recent years, mechanochromic or piezochromic luminescent materials which exhibit reversible modification of the emission wavelength in response to external mechanical forces (grinding, shearing, compressing, or rubbing) have attracted much intention because of their potential applications in optical recording/memory devices, pressure or motion sensing systems, and damage detectors, for instance.[4−13] Indeed, due to their promising development, the number of reported pressure-sensitive luminescent compounds has exploded in the five last years with examples based on transition-metal complexes[14] still relatively limited compared to the organic molecule ones.[15] Concerning metal-based compounds, examples reported so far[16−21] are mainly based on gold[22] and platinum[23] complexes. We have reported recently the first example of a mechanochromic luminescent complex based on copper.[24] This compound is actually a molecular copper iodide cluster formula $[Cu_4I_4(PPh_2(CH_2CH{=}CH_2))_4]$ whose photoemission properties are modified upon mechanical grinding, thus exhibiting both mechanochromic and thermochromic luminescence properties. The thermochromic luminescence properties are characterized by the reversible change of the emission wavelength with the temperature. The origin of the mechanochromism has been attributed to structural changes of

Received: January 9, 2014
Published: July 30, 2014

   dx.doi.org/10.1021/ja500247b | J. Am. Chem. Soc. 2014, 136, 11311−11320

the $[Cu_4I_4]$ cluster core geometry, in particular of the Cu−Cu interactions, thus influencing the emissive states. This assumption was based on hypothesis because no direct proof of the Cu−Cu bond contraction in the crushed compound could be obtained at the time. Since then, a few other examples of copper-based mechanochromic luminescent complexes have been reported in the literature,[25] and similar conclusions have been established.

To design and develop new stimuli-responsive materials with intriguing properties, an in-depth understanding of the underlying mechanisms is highly demanded. Indeed, the determination of the mechanism involved in the mechanochromic phenomenon is always a big issue. The major difficulty is that the origin of the mechanochromic properties is system dependent without a general rule. Different hypotheses have been advanced, but a molecular-level understanding of the mechanochromic mechanisms often remains unclear without direct proof. However, as the solid-state emission strongly depends on the molecular structure and arrangement in the solid state via intermolecular interactions, it is usually accepted that the mechanical grinding subtly alters the structural packing mode and thus modifies the emitting wavelength.[26] To know precisely the structural change that occurs at the molecular level, single crystal X-ray diffraction is the method of choice due to its easy and readily accessibility but is usually inapplicable because the grinding process leads generally to amorphous compounds. To elucidate the origin of the mechanochromism, it is thus essential to achieve a molecular-level understanding of the relationship between the molecular packing characteristics and the resulting optical properties.

A crystalline polymorph of a molecular solid is a solid crystalline phase of a given compound resulting from the possibility of at least two different arrangements of the molecules of that compound in the solid state.[27] When there are no significant electronic interactions between the molecules, the optical properties of the polymorphic solid reflect the optical properties of the individual molecules. In particular, crystalline polymorphs of luminescent molecular compounds usually show different emissions properties, and their study can give straightforward correlation between the molecular structure and the optical properties.[28−32] Such correlations have been established for several transition-metal compounds such as the well-known Alq_3 (tris(8-hydroxyquinoline)-aluminum(III)) complex for which interligand contacts are involved.[33] Other particularly relevant examples are compounds for which luminescence changes arise from modifications of metal−metal interactions, as previously reported for gold[34] or platinum[35] complexes. In this context, obtaining crystalline polymorphs of a mechanochromic luminescent complex appears an efficient approach to elucidate the factors responsible for the mechanochromism. In this vein, scarce examples have been reported in the literature for organics[36] and even less for metal-based compounds[20a,21a,22j,23f] for which correlation between structural and optical properties has been established to explain the mechanochromism mechanism observed. Thus, different molecular conformations of the ligands, induced by changes in intermolecular interactions, have been reported to be responsible for the mechanochromic properties of aluminum and iridium complexes.[20a,21a] Variation of metallophilic interactions has been also reported for platinum[23f] and gold[22j] complexes.

Here, we report on an in-depth study of a new mechanochromic and thermochromic luminescent copper iodide cluster, giving new insights into the mechanochromic luminescence properties of this family of compounds. The studied cluster formula $[Cu_4I_4(PPh_2(CH_2)_2(CH_3)_2SiOSi(CH_3)_2(CH_2)_2PPh_2)_2]$ (**1**) presents two different crystalline polymorphs exhibiting distinct luminescence properties with one being green emissive (**1G**) and the other one being yellow emissive (**1Y**) at room temperature (Chart 1). Upon mechanical grinding, only the **1G** polymorph exhibits great modification of its solid-state luminescence properties with its room temperature emission changing from green to yellow. Interestingly, the photophysical properties of this new yellow emissive crushed phase (**1C**), which is partially amorphous, are close to those of the yellow polymorph (**1Y**), and comparative structural and optical analyses of the three forms (**1G**, **1Y**, **1C**) including a solution of clusters (**1S**) provide precious clues into the origin of luminescence mechanochromism. In particular, the local structure of the $[Cu_4I_4P_4]$ cluster cores has been probed by solid-state NMR (nuclear magnetic resonance), and analysis of the cluster before and after the grinding process readily indicates modification of the copper and phosphorus atoms environments. The mechanochromic phenomenon is explained by disruption of the crystal packing within the intermolecular arrangement, inducing contraction of the Cu−Cu distances in the $[Cu_4I_4]$ cluster core and eventually modification of the emissive state. This study constitutes a step further into the understanding of the mechanism involved in the mechanochromic luminescent properties of copper iodide clusters and more generally of metal-based compounds.

Chart 1. Designation of the Clusters Studied

$[Cu_4I_4(PPh_2(CH_2)_2(CH_3)_2SiOSi(CH_3)_2(CH_2)_2PPh_2)_2]$	**1**
Yellow emissive polymorph	**1Y**
Green emissive polymorph	**1G**
Crushed green emissive polymorph	**1C**
Cluster in solution in dichloromethane	**1S**

RESULTS

Polymorphism. The rich photoluminescence properties of the copper iodide clusters are particularly attractive to synthesize materials with original optical applications. In this context, we have reported hybrid sol−gel materials exhibiting thermochromic luminescence properties by incorporating $[Cu_4I_4L_4]$ clusters coordinated by phosphine ligands in a silica matrix.[37,38] We have studied the functionalization of the clusters with alkoxysilane ligands to covalently graft the cluster to the silica sol−gel network. During the course of these investigations, we were thus interested in synthesizing clusters coordinated with alkoxysilane phosphine-based ligands such as $PPh_2(CH_2)_2Si(CH_3)_2(OCH_2CH_3)$.

By reacting copper iodide with this alkoxysilane phosphine ligand in solution, the cubane cluster $[Cu_4I_4(PPh_2(CH_2)_2(CH_3)_2SiOSi(CH_3)_2(CH_2)_2PPh_2)_2]$ (**1**) is formed (Supporting Information). The reaction thus occurring is schematically represented in Figure 1 with the ligand becoming chelating through the formation of Si−O−Si bridges resulting from the hydrolysis followed by intracluster condensation of the $SiOCH_2CH_3$ groups. The hydrolysis−condensation of the ligand required water molecules which come from the use of undried solvents. Recrystallization of **1** gave colorless crystals which surprisingly exhibit two different

dx.doi.org/10.1021/ja500247b | J. Am. Chem. Soc. 2014, 136, 11311−11320

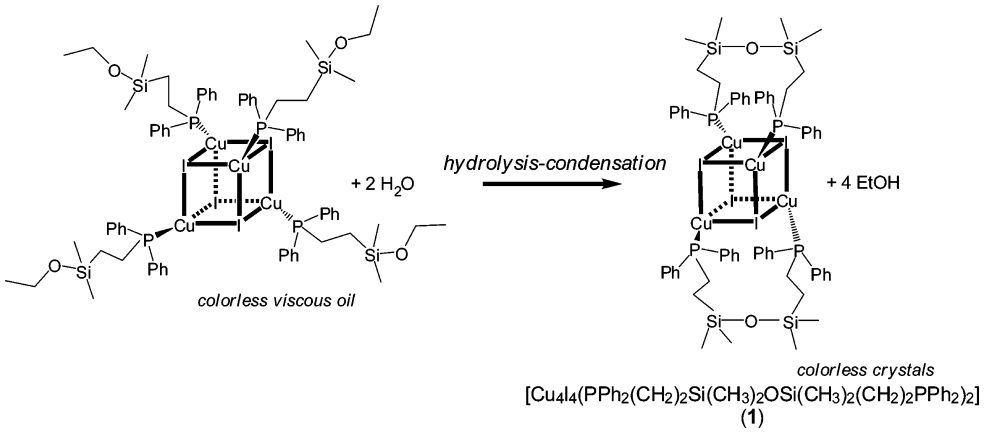

Figure 1. Synthesis of cluster **1** from the hydrolysis and condensation of the alkoxysilane ligand.

colors under UV: some of them present a green emission while others emit a yellow light as shown in Figure 2.

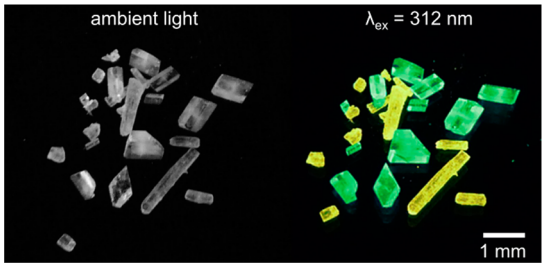

Figure 2. Photos of the polymorphic crystals of **1** under ambient light and under UV irradiation at 312 nm (UV lamp) at room temperature.

The two different crystalline polymorphs show an intense and distinctive emission which allow their easy and manual separation under a UV lamp. Their respective crystal structures were solved by single crystal X-ray diffraction analysis (Table S1, Supporting Information). The two compounds are composed of the same cluster formula $[Cu_4I_4(PPh_2(CH_2)_2(CH_3)_2SiOSi(CH_3)_2(CH_2)_2PPh_2)_2]$ (**1**) which crystallizes in different space groups. The green luminescent polymorph (**1G**) crystallizes in monoclinic *C*2/*c* whereas the yellow one (**1Y**) crystallizes in triclinic *P*-1 with chloroform solvent molecules included ($[Cu_4I_4(PPh_2(CH_2)_2(CH_3)_2SiOSi(CH_3)_2(CH_2)_2PPh_2)_2]\cdot(CHCl_3)_{0.5}$). Note that **1G** and **1Y** are more accurately pseudopolymorphs because their composition differs from solvent molecules. The unit cell contents are shown in Figures S1, Supporting Information. Both structures can be described as an assembly of columns of clusters. The columns run along the *b* axis for **1G** and along the *a* axis for **1Y**. In the latter, the cluster orientation changes alternatively from one column to the other due to the two independent clusters in the asymmetric unit (1Ya and 1Yb).

The molecular structures of the clusters in **1G** and **1Y** are depicted in Figure 3. The clusters present a cubane structure formed by four copper atoms and four iodine atoms which occupy alternatively the corners of a distorted $[Cu_4I_4]$ cube. The phosphine ligands are coordinated to each copper atom by the phosphorus atom. As expected, the hydrolysis and condensation reactions of the alkoxysilane $SiOCH_2CH_3$ group of two different ligands result in the formation of two intracluster siloxane Si−O−Si bonds. Formulations for the clusters are in agreement with NMR (^1H, ^{31}P, and ^{29}Si), elemental analysis, and FTIR. In particular, the Si−O bond vibration appears as a broad band centered at 1050 cm^{-1} along with the Si-CH_3 and Si-CH_2 related peaks at 785 and 1256 cm^{-1}, respectively (spectrum in Supporting Information).

Selected bond lengths and angles of the clusters are listed in Table S2, Supporting Information, and mean values are reported in the caption of Figure 3. In both **1G** and **1Y**, the siloxane bond presents the expected values for the Si−O distance in the range 1.609−1.641(1) Å as well as values for the Si−O−Si angle (146.49−168.48(1)°). There are slight differences in the Cu−I and Cu−P bond distances in clusters **1G** and

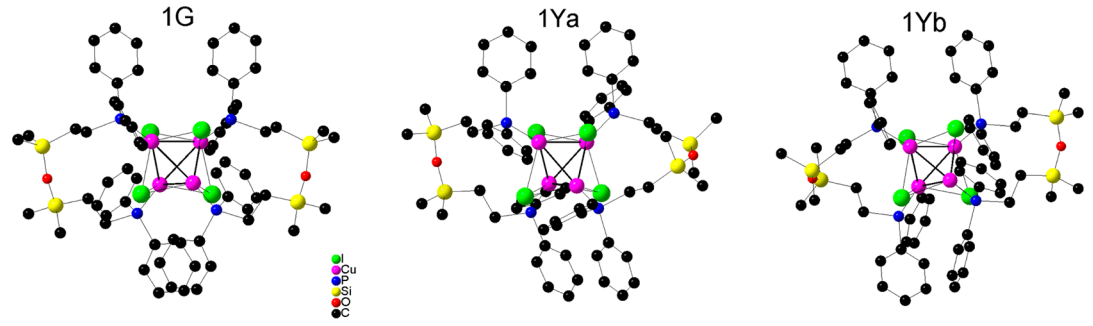

1G : Cu-Cu : 3.104(1), Cu-I : 2.697(1), Cu-P : 2.252(1) Å and I-Cu-I : 106.69(2)°.

1Ya : Cu-Cu : 2.953(1), Cu-I : 2.698(1), Cu-P : 2.257(1) Å and I-Cu-I: 109.01(4)°

1Yb : Cu-Cu : 2.816(1), Cu-I : 2.693(1), Cu-P : 2.254(1) Å and I-Cu-I: 111.13(3)°

Figure 3. Molecular structure of clusters **1G** and **1Y** and the mean of selected bond lengths. Hydrogen atoms have been omitted for clarity.

dx.doi.org/10.1021/ja500247b | J. Am. Chem. Soc. 2014, 136, 11311−11320

1Y, but those values are within the range of those reported for copper iodide clusters coordinated with phosphine derivatives. The Cu−Cu distances are also within the range of reported values for diphenylphosphine ligands, but they are significantly longer for cluster **1G** with a mean distance of 3.104(1) Å compared to those of the two crystallographic independent clusters in **1Y** of 2.953 (1) Å and 2.816(1) Å. These Cu−Cu values are close to the sum of the van der Waals radii of copper(I) (2.80 Å) and imply different cuprophilic interactions for the clusters in the two polymorphs.[39]

Concerning the intercluster interactions, short CH···H contacts less than 3.1 Å exist in **1G** between the phenyl groups and the methyl groups even down to 2.8 Å. Weak O···HCH_2 hydrogen bonds occur between oxygen atoms of the siloxane bridge and hydrogen of the methyl groups. In **1Y**, there are several CCl···H contacts between the incorporated solvent and the phenyl groups of the ligands, and multiple CH···H (<3 Å) contacts are also present between the methyl or methylene groups and the phenyls. Note that despite the presence of several phenyl groups, no $\pi-\pi$ stacking is observed in both structures (Figures S2 and S3, Supporting Information).

Mechanochromic Luminescence. Cluster **1G** exhibits mechanochromic luminescence properties whereas **1Y** does not. Grinding the solid sample (**1G**) using a pestle in an agate mortar leads to a dramatic change in the emission color: the initial green emission is converted into a yellow one while the color of the powder remains white (Figure 4).

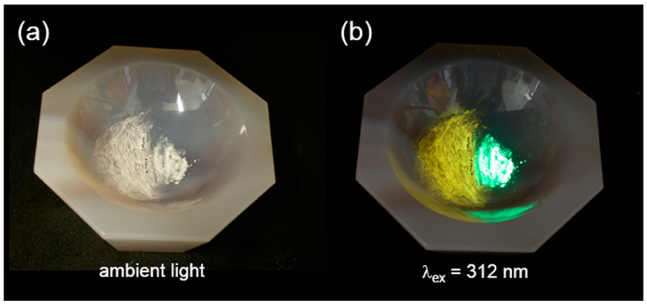

Figure 4. Photos of the ground (left) and intact (right) crystalline powder of **1G** (a) under ambient light and (b) under UV irradiation at 312 nm (UV lamp) at room temperature.

Elemental analyses of the compound before (**1G**) and after grinding (**1C**) both gave the expected composition (based on the formula $[Cu_4I_4(PPh_2(CH_2)_2(CH_3)_2SiOSi(CH_3)_2(CH_2)_2PPh_2)_2]$, see Supporting Information), indicating that no chemical reaction related to adsorption or removal of atmospheric molecules was induced by the grinding. ^{31}P and ^{1}H liquid NMR, UV−vis absorption (λ_{max} = 300 nm, Figure S6, Supporting Information), and luminescence spectra in solution at room temperature (λ_{max} = 595 nm at λ_{ex} = 300 nm, Figure 9) are similar whether the cluster is crystalline or crushed before its dissolution, showing that the molecular structure of the cluster is preserved in the crushed powder. This is further confirmed by the luminescence thermochromism exhibited by the crushed compound (**1C**) which is typical of $[Cu_4I_4L_4]$ clusters as described in the following part. The powder X-ray diffraction (PXRD) analysis of **1G** revealed numerous sharp and intense diffraction peaks which indicate good crystallinity (Figure 5). The peaks correspond to those calculated from the data of the single crystal diffraction analysis, confirming the purity of the powdered sample (Figure S5, Supporting Information). After grinding, there is no distinct diffraction peak anymore, indicating significant damage to the crystalline packing that leads to an almost complete amorphous state.

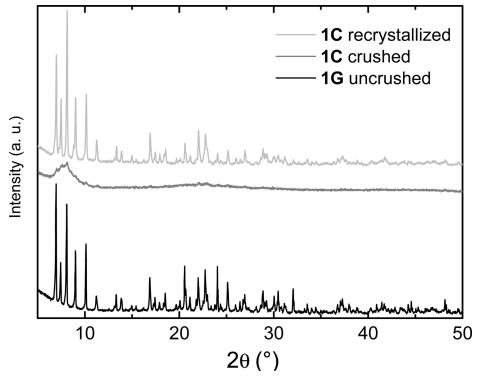

Figure 5. PXRD (Cu Kα) recorded at room temperature of **1** before (**1G**) and after grinding (**1C**) and after recrystallization in ethanol (**1C**).

The compound recovers its original crystalline phase (**1G**) and emission properties upon exposure of the crushed powder to vapor or liquid ethanol (Figure 5). This effect is quite surprising because the compound is not soluble in this solvent and thus cannot be attributed to a classical recrystallization phenomenon. Indeed, when the powder is placed in the liquid, it does not readily dissolve, and the liquid phase does not display any trace of luminescence; therefore, if the compound is soluble, it is only soluble at very low concentrations. The amorphous yellow emissive powder is recovered when the solid is ground one more time, which indicates a completely reversible phenomenon (at least four times). Note that heating the **1C** sample at different temperatures and durations does not result in the regeneration of the green emissive **1G** phase. This is contrary to the case of many other mechanochromic compounds, which after grinding, revert back to their original phases upon treatment with heat.[14,15]

Local Structure of the $[Cu_4I_4P_4]$ Cluster Cores. The studied cluster $[Cu_4I_4(PPh_2(CH_2)_2(CH_3)_2SiOSi(CH_3)_2(CH_2)_2PPh_2)_2]$ (**1**) presents several NMR nuclei such as ^{31}P and $^{63,65}Cu$, which are particularly useful for probing the $[Cu_4I_4P_4]$ cluster core in the different structures. The ^{31}P solid-state CPMAS NMR spectra for **1G**, **1C**, and **1Y** are reported in Figure 6. At first sight, the spectrum of **1G** contains more patterns than the two expected from the two independent P sites in the crystal structure. In fact, it can be understood, taking

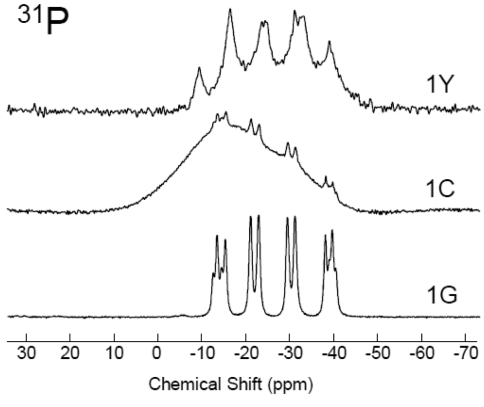

Figure 6. ^{31}P CPMAS NMR spectra of **1G**, **1C**, and **1Y**.

dx.doi.org/10.1021/ja500247b | J. Am. Chem. Soc. 2014, 136, 11311−11320

into account the one-bond *J*-couplings between the ^{31}P and the two copper isotopes (^{63}Cu, with 30.8% natural abundance and ^{65}Cu, with 69.2% natural abundance, both having a nuclear spin value of 3/2) and the residual dipolar coupling.[40−43] The spectrum can therefore be deconvoluted with two ^{31}P patterns of similar intensity (Figure S9, Supporting Information), each of them being split into two quartets with the $^{31}P-^{63}Cu$ (1660 and 1670 for the two sites) and $^{31}P-^{65}Cu$ (1790 and 1750 Hz for the two sites) ^{1}J-coupling constants (see Supporting Information). For **1C**, the ^{31}P NMR spectrum contains a broad pattern which overlaps with a contribution of smaller intensity that is similar to the pattern of **1G**. The presence of an unstructured signal confirms that the grinding process has induced amorphization of the solid, along with a distribution of the phosphorus environment. The remaining contribution similar to the signal of **1G** indicates that the amorphization is not complete in accordance with the PXRD analysis. The center of the broad contribution is also shifted to higher field (∼−18 ppm) compared to **1G** (−26 ppm), indicating a modification of the P environment upon grinding. The spectrum of **1Y** is centered at −25 ppm and, although less resolved because there are eight different Cu−P bonds in the small range 2.251(1)−2.262(1) Å for the two independent clusters in the structure, the characteristic quartets due to the $P-^{63,65}Cu$ *J*-couplings can still be distinguished. These data show that each compound has a different ^{31}P signature resulting from different phosphorus atoms in their structures and further clearly indicate that the grinding process modifies the phosphorus environment in the cluster and most probably the P−Cu bond characteristics.

The more exotic ^{65}Cu NMR nucleus has been also studied, which is particularly appealing, as it gives direct information about the local environment of the copper atoms and hence the cuprophilic interactions in the clusters which are supposed to be involved in the mechanochromism. ^{65}Cu is sensitive and reasonably abundant (30.8%) but has a large quadrupolar moment, resulting in particularly broad ^{65}Cu NMR spectra, that can extend over a few MHz.[43−47] Static ^{65}Cu solid-echo NMR spectra were recorded for compounds **1G** and **1C** (Figure 7), but the amount of **1Y** was too low to record a ^{65}Cu spectrum. The ^{65}Cu NMR signatures of **1G** and **1C** are clearly distinct, confirming that the grinding process has significantly modified the $[Cu_4I_4P_4]$ cluster core. For comparison, the spectra of the prototypical $[Cu_4I_4(PPh_3)_4]$[48] cluster has also been recorded (Figure 7).

To assist the analysis of the NMR spectra, DFT calculations at the PBE0/Def2-TZVP level (see experimental section in SI) were run on **1G** and $[Cu_4I_4(PPh_3)_4]$ clusters, using the structural data determined from single-crystal X-ray diffraction, except for the hydrogen atoms which were relocated at calculated positions. For both compounds, a reasonably good agreement is obtained between the DFT-calculated and the experimental NMR spectra (Figures S13 and 14, Supporting Information), validating the structural models, in particular the presence of the two crystallographically inequivalent Cu sites in **1G** (Cu1 and Cu2 in Table S2, Supporting Information). The spectra of the latter compound is thus composed of two patterns (Figure 7) which are assigned unambiguously on the basis of the DFT calculations to Cu1 and Cu2. From these results, the NMR parameters were then refined (see Supporting Information), and the best fit is shown in Figure 7. One can notice the similarity between the pattern of Cu2 of **1G** and the NMR spectrum of $[Cu_4I_4(PPh_3)_4]$. The ^{65}Cu NMR spectrum

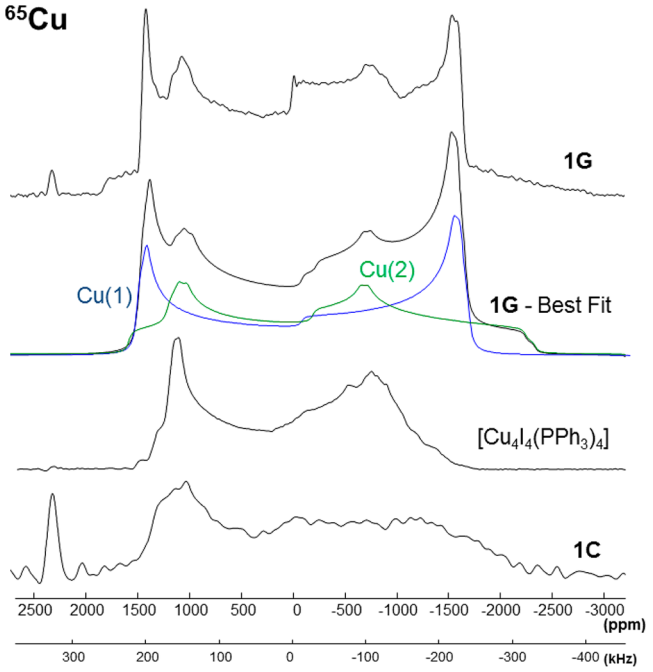

Figure 7. Experimental solid-state static ^{65}Cu NMR spectra of **1G**, $[Cu_4I_4(PPh_3)_4]$, and **1C**. The best fit of the **1G** spectrum, performed starting from the DFT results, is shown along with the individual contributions of Cu1 and Cu2 sites. The peaks at 2400 ppm are the copper signal of the NMR coil.

of the ground compound **1C** is shown in Figure 7. The pattern is broad, which is a characteristic result of amorphization. The shape of the spectrum is quite similar to that of Cu2 in the parent compound **1G** and to the spectrum of $[Cu_4I_4(PPh_3)_4]$ (Figure 7). However, the spectrum of **1C** no longer contains the resonance Cu1 of the parent compound. These spectrum changes indicate that a modification of the local environment of at least one of the Cu sites of the parent compound has occurred during grinding. The shape of the ^{65}Cu pattern is mostly influenced by the nearest neighbors, which define the local geometry around the Cu atoms: Cu−I and Cu−P bond lengths, I−Cu−I bond angles, and thus, indirectly, Cu−Cu distances. One can notice, based on X-ray diffraction data, that the cluster core in **1G** is much more distorted compared to that in $[Cu_4I_4(PPh_3)_4]$. Indeed, the geometrical characteristics of the two Cu sites in **1G** vary more than in $[Cu_4I_4(PPh_3)_4]$, whose four Cu sites have more similar environments (Table S2, Supporting Information). This results in a ^{65}Cu NMR spectrum of **1G** that contains two well distinct powder patterns, while in the $[Cu_4I_4(PPh_3)_4]$ cluster, the four individual components can hardly be distinguished (the quadrupolar parameters present small variations as reported in Table S4, Supporting Information). As mentioned above, the spectrum of **1C** is similar to the Cu2 pattern only of **1G** and also to the spectrum of $[Cu_4I_4(PPh_3)_4]$. This indicates that the amorphization induced by the grinding has reduced the differences between the local geometries of the various Cu sites in **1C**, which in turn indicates that the cluster cores have less distorted geometries after grinding (the Cu sites in **1C** have less variations in their local environments, such as in $[Cu_4I_4(PPh_3)_4]$, opposite to the two components in the parent compound **1G**). In agreement with the other characterizations (vide infra), these changes can be associated with a Cu−Cu bond shortening.

dx.doi.org/10.1021/ja500247b | J. Am. Chem. Soc. 2014, 136, 11311−11320

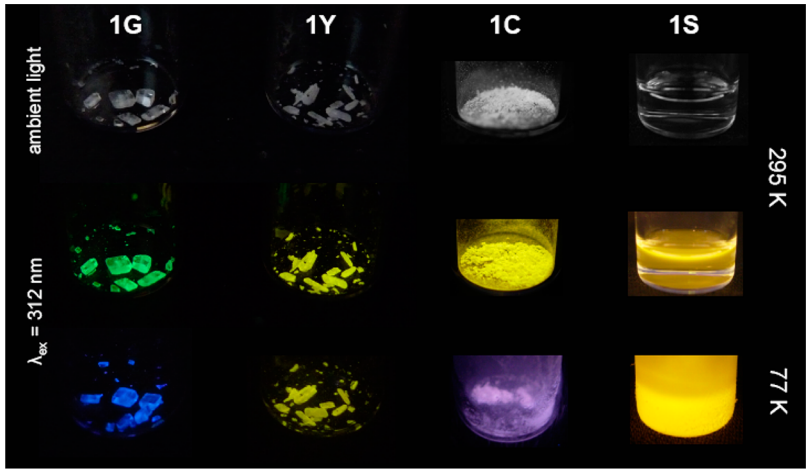

Figure 8. Photos of **1G**, **1Y**, **1C**, and **1S** clusters under ambient light and UV irradiation at 312 nm (UV lamp) at room temperature (295 K) and in liquid nitrogen (77 K).

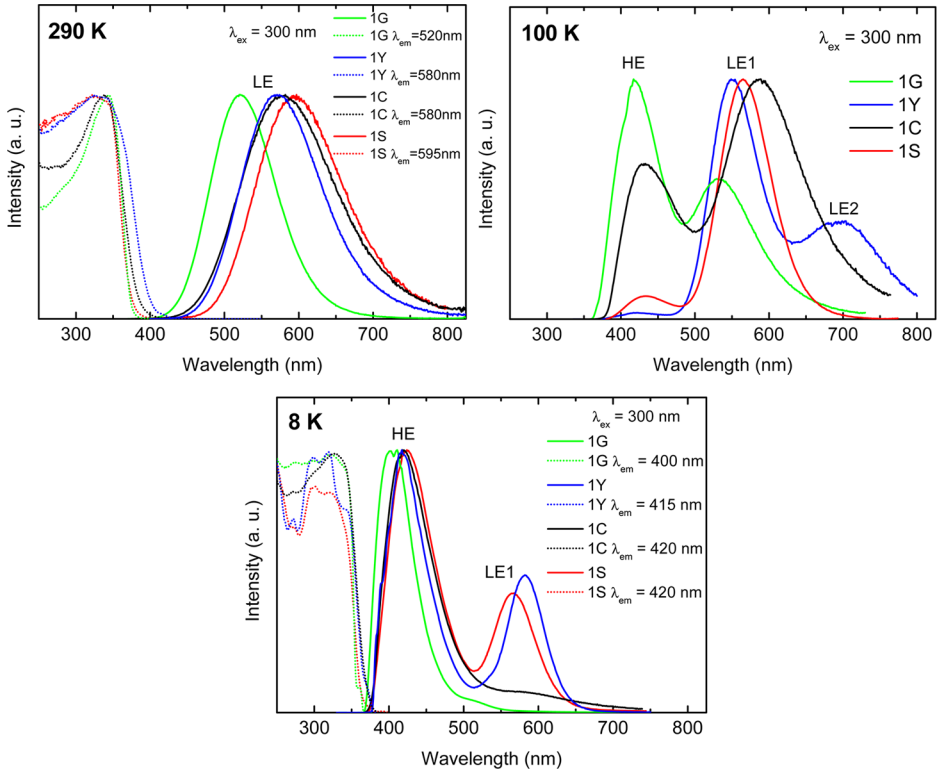

Figure 9. Temperature dependence of luminescence spectra of **1G**, **1Y**, **1C**, and **1S**: normalized emission (solid lines λ_{ex} = 300 nm) with corresponding excitation spectra (dotted lines) at 290, 100, and 8 K.

The ^{29}Si CPMAS NMR spectra of **1G** and **1C** have also been recorded (Figure S10, Supporting Information). The signal of **1G** centered at 8.5 ppm presents two doublets resulting from the two independent silicon atoms in the structure, the signals being split due to coupling with the nearest phosphorus atom. The signal of **1C** presents a similar chemical shift with a clearly less structured signal. As for the ^{31}P and ^{65}Cu nuclei, the NMR patterns are broader, indicating almost complete amorphization of the compound upon grinding. However, for the ^{29}Si nucleus, the isotropic chemical shifts did not vary between the **1G** and **1C** compounds, demonstrating that the ligand structure is not significantly affected by the grinding process.

Thermochromic Luminescence. The polymorphism and mechanochromism induce different thermochromic luminescence properties of the clusters. When crystals of **1G** and **1Y** are dipped in liquid nitrogen (77 K), their emission colors change differently as shown in Figure 8. Under UV excitation, the room temperature green emission of **1G** is replaced by a blue one whereas the yellow color of **1Y** does not change much. The grinding process also affects the thermochromic luminescence properties of the cluster. The room temperature yellow emission of the **1C** crushed compound turns into purple at 77 K that is different from the blue one exhibited by the pristine crystalline **1G** cluster (Figure 8). For the cluster in solution in dichloromethane **1S**, the room temperature yellow

dx.doi.org/10.1021/ja500247b | J. Am. Chem. Soc. 2014, 136, 11311−11320

emission is almost unchanged in the frozen state like that for **1Y** (77 K). When the samples are progressively warmed to room temperature, the initial emissions are recovered, indicating a completely reversible thermochromic luminescence behavior for all of them.

Solid-state emission and excitation spectra have been recorded for clusters in the different states (**1G**, **1Y**, **1C**, and **1S**) from room temperature down to 8 K (Figure 9 for 290, 100, and 8 K and Figure S7, Supporting Information, for other temperatures). Corresponding data are reported in Table S3, Supporting Information. At 290 K, the emission spectra (λ_{ex} = 300 nm) display a single unstructurated broad emission band (LE = low energy) centered at 522 nm for **1G** which greatly shifts to 578 nm after the grinding process (**1C**). This red shift of more than 50 nm is among the largest reported for mechanochromic compounds. The yellow polymorph **1Y** also emits a yellow luminescence with a maximum at 571 nm. When the cluster is dissolved in solution, its emission is red-shifted to 595 nm (**1S**). The excitation profiles are quite similar for all the samples with maxima around 330 nm. The internal absolute quantum yields of the clusters have been determined at room temperature, and the values obtained with excitation at 300 nm are 62%, 67%, 29%, and 32% for **1G**, **1Y**, **1C**, and **1S**, respectively. Emission lifetimes have been determined at 290 K, and the corresponding decays are reported in Figure S8, Supporting Information. The emission lifetime values of **1G**, **1Y**, and **1S** are 2.6, 6.1, and 0.4 μs, respectively. Whereas those data present single exponential decays, the data recorded for **1C** are best fitted with a biexponential decay with τ_1 = 1.0 μs and τ_2 = 4.9 μs.

By lowering the temperature, a new emission band appears at higher energy (HE = high energy) for clusters **1G** and its crushed form **1C** (Figure 9 and Figure S7, Supporting Information) that is typical of the thermochromic luminescence properties of copper iodide cubane clusters.[49] This new band progressively increases in intensity with the concomitant extinction of the lower energy band (LE) without significant shift of their positions. At 100 K, the two emission bands are present with maxima at 419 and 533 nm for **1G** and at 433 and 587 nm for **1C** with excitation profiles similar to those at 290 K. The addition of the yellow and blue lights gives the purple emission observed for **1C** in liquid nitrogen (77 K) whereas the cluster **1G** emits bluer (Figure 8) because of the relative larger contribution of the HE band at this temperature. At 8 K, the blue band (HE) is largely dominant at 404 nm for **1G** and at 420 nm for **1C** with similar excitation profiles having maxima at 330 nm. For cluster **1Y**, the situation is more complex because in addition to the new HE band another one at lower energy (LE2) first appears during the cooling. At 100 K, the LE2 band is centered at 700 nm whereas the LE1 band (initial at RT) is centered at 550 nm (similar excitation profiles), and at 75 K, the three bands, blue (HE), yellow (LE1), and red (LE2), are simultaneously present (at 419, 578, and 711 nm, respectively). At lower temperature, the LE2 band progressively disappears at the expense of the HE band. At 8 K, the LE1 band that shifted to 582 nm is still present along with the HE band at 420 nm, opposite to that observed for **1G** and **1C**. This explains that the sample keeps its yellow emission at lower temperature compared to the other ones; the thermochromism is only visible below the liquid nitrogen temperature when the blue HE band has a significant intensity (Figure 8). The luminescence thermochromism properties of the cluster in solution **1S** are very similar to those of **1Y**. The only difference is the lack of the second low energy band LE2. At 100 K, the HE starts to appear at 432 nm with the LE band centered at 565 nm. At 8 K, the latter is still present as for **1Y**. The excitation profiles of the HE emission bands are also similar for **1S** and **1Y**.

DISCUSSION

The luminescence origin of the phosphine-based $[Cu_4I_4L_4]$ copper iodide clusters has been established based on experimental and theoretical data (DFT calculations).[48] In particular, the thermochromism exhibited by these clusters, that is the variation in temperature of the relative intensities of two emission bands (LE and HE), derives from the thermal equilibrium of the two related excited states which have different natures (Figure S10, Supporting Information).[50,51] The broad green-yellow emission (LE) observed at room temperature is assigned to a $[Cu_4I_4]$ cluster centered excited state called "cluster centered" (^{3}CC) and is essentially independent of the nature of the ligand. This triplet excited state is a combination of a halide-to-metal charge transfer (XMCT) and copper-centered 3d → 4s, 4p transitions. In contrast, the blue band appearing at higher energy (HE), during cooling, is "ligand-centered" with a mixed charge-transfer (MLCT/XLCT) triplet excited state. Due to the nature of the LE band, the emission can be correlated to interatomic distances in the $[Cu_4I_4]$ cluster core. Indeed, this LE emission corresponds to a transition from a Cu−Cu nonbonding and Cu−I bonding HOMO to a strongly Cu−Cu bonding and Cu−I antibonding orbital (the LUMO+24 in $[Cu_4I_4(PPh_3)_4]$).[48] This leads, upon excitation, to a strong geometrical relaxation of the ^{3}CC state relative to the ground state due to electron redistribution into a Cu−Cu bonding state. This transition is thus accompanied by distortions of the $[Cu_4I_4]$ core with an increase of Cu−I and an important decrease of Cu−Cu distances with respect to the ground state. This phenomenon is revealed by the large Stokes shift observed. It is interesting to note that even clusters having Cu−Cu bond distances longer than the 2.8 Å van der Waals contact value of Cu(I) exhibit this emissive CC state.[44−46]

The different luminescence properties observed for cluster **1** in different states can be thus correlated to differences in the molecular structures and especially in the geometries of $[Cu_4I_4]$ clusters cores. For the LE band, the distortion (relaxation after excitation) can be considered similar for the different clusters (similar environment in solid state); therefore, the energy of the states mainly depends on the Cu−Cu interactions with shorter distances leading to stabilization of the emissive state. From the crystallographic structures, the green emissive **1G** cluster presents longer Cu−Cu distances compared to its yellow polymorph **1Y** whereas their Cu−I bonds are similar. This explains that the emission is of higher energy for the green **1G** cluster compared to the yellow **1Y** cluster. This is in agreement with previous studies for which a red shift of the LE band upon cooling has been correlated to the decrease of the Cu−Cu distances.[52] A similar correlation has been reported to explain the luminescence difference of $[Cu_4I_4(PPh_3)_4]$ polymorphs.[53] Whereas **1G** and **1C** present a classical thermochromism for copper iodide clusters with the LE and HE bands, the presence of a third band (LE2) for **1Y** is unprecedented to our knowledge. By analogy, the two LE bands can be easily attributed to the two independent clusters in the asymmetric unit of the crystal structure having different $[Cu_4I_4]$ core geometries. The cluster with the shorter Cu−Cu bonds leads to the redder emission band (LE2). This agrees

dx.doi.org/10.1021/ja500247b | J. Am. Chem. Soc. 2014, 136, 11311−11320

with the cluster in solution **1S** exhibiting similar behavior but with only one LE band. The single LE emission band observed at 290 K for **1Y** must be composed of the two emissions from the two independent clusters, in accordance with the larger bandwidth compared to **1G**. At this temperature, their molecular structures do not lead to significant different emissions. At low temperature, only one HE band is observed for **1Y** which corresponds to the two clusters because this band involves the ligand that is identical.

Through the correlation between the Cu−Cu distances and the emission of the copper iodide clusters being established, information can be obtained concerning the origin of the mechanochromic luminescence properties. Upon mechanical grinding, the green emission of **1G** is converted into a yellow one which is very similar to that of the yellow polymorph **1Y**. This implies that the molecular structure of the amorphous compound **1C** is similar to that of **1Y** and therefore that the grinding process induces reduction of the Cu−Cu bond lengths (without altering the cluster integrity). Note that the emission bandwidth (LE) is slightly broader for **1C** compared to that for **1Y**, the latter being even broader than that for **1G**, meaning that the grinding induces to some extent a distribution of cluster core geometries. This is in accordance with the appearance of two different emission lifetimes. These results are further confirmed by probing the local structure of the cluster cores by solid-state NMR, which clearly shows different ^{31}P and ^{65}Cu spectra for the cluster before and after grinding (**1G** and **1C**) and thus modification of the copper and phosphorus atom environments. From these data, combined with luminescence and X-ray diffraction results, modifications of the $[Cu_4I_4]$ cluster core geometries occur upon the grinding process, which are associated with the formation of a less distorted $[Cu_4I_4]$ core with most probably shorter Cu−Cu bonds. The NMR study also confirmed the almost complete amorphization of the crushed compound, leading to a distribution of cluster geometries to some extent. A mechanism involving a shortening of the Cu−Cu bonds agrees with the molecular structure of cluster **1G** presenting relatively long Cu−Cu distances compared to known phosphine-based clusters (up to 3.329(1) Å). Therefore, **1G** seems to crystallize in a somehow constrained molecular structure. The luminescence properties of the cluster in solution **1S**, without constraints, exhibiting a yellow LE emission band support this statement. Study of the crystalline environment of the clusters in **1G** and **1Y** revealed relatively weak intercluster interactions with no specific interaction and especially none directly involved the $[Cu_4I_4]$ core. This is in accordance with the concomitant crystallization of the two polymorphs that implies a small energy difference. This also explains that these interactions can be easily disrupted by the grinding process, leading to almost complete amorphization of the compound. Once the crystalline lattice collapses, the cluster relaxes to a more symmetrical geometry with shorter Cu−Cu bonds and thus emits redder emission.

Compared with other mechanochromic compounds, the transformation from a crystalline phase to an amorphous state is the most common feature of mechanochromism but it is not systematic.[14,15] In particular, the previously reported cluster $[Cu_4I_4(PPh_2(CH_2CH{=}CH_2))_4]$ only shows an increase in the diffraction peak width upon grinding.[24] This means that the intercluster interactions are in the present case (**1G**) weaker. Aside from the shifting, the luminescence quantum yield is usually decreased when the compound is ground. This is the case for cluster **1** but again differs from the previously reported cluster. However, in both cases, the cuprophilic interactions play a crucial role in the mechanochromism because a bathochromic shift of the emission is still observed. The involvement of metal−metal interactions in the mechanochromism mechanism is common with other metal-based complexes based on gold[22] and platinum.[23h] For most of those cases, the metallophilic interactions involve independent complexes because they are mononuclear. This can be correlated to the mechanochromic organic molecules for which intermolecular interactions (H-bonds, $\pi-\pi$ stacking, etc.) usually play a more important role than intramolecular ones. This differs from our case in which metal−metal interaction modulations occur within a single molecular cluster. However, although weak, the intercluster interactions observed in the polymorphic structures are slightly different, showing that subtle changes in the cluster interactions lead to important Cu−Cu bond variations and great luminescence modifications. The competition between the collective intercluster interactions (crystalline cohesion) and the individual intracluster interactions appears to be the key parameter in the mechanochromic phenomenon.

CONCLUSION

Controlling or tuning the photoluminescence properties by means of external stimuli is particularly attractive to obtain photofunctional materials. Although numerous examples of mechanochromic compounds have been reported in the literature, an in-depth theoretical understanding of the phenomena has rarely been conducted although it is crucial for the development of such materials. In this study, copper iodide clusters exhibiting mechanochromic luminescence properties and structural polymorphism have been reported. Detailed photophysical investigations and especially correlation between structural (X-ray diffraction, solid-state NMR) and optical properties of the polymorphic phases provide deep insights into the mechanochromism phenomena. Variations of intermolecular interactions in the cluster packing induce great changes in the luminescence properties, and this study clearly establishes that Cu−Cu interactions are directly responsible. More precisely, upon mechanical stimulation, destruction of the crystalline interactions leads to Cu−Cu bond shortening in the cluster core. These results definitely establish the role of cuprophilic interactions in the mechanochromic mechanism of copper iodide clusters.

The studied mechanochromic compounds show promising applicability. Indeed, upon grinding, a dramatic shift in the emission color is observed along with a noticeable luminescence efficiency variation, allowing a high contrast ratio which is important for the applications. The grinding also affects the thermochromic luminescence properties of the compounds which then represent a rare example of a mechanoswitchable compound combining both mechanochromic and thermochromic luminescence properties. It is important to note that these mechanochromic and thermochromic luminescence properties are reversible and readily detectable by the naked eye, thus rendering such stimuli-responsive solid emitters appealing as smart materials. In addition, mechanochromic materials based on copper metal present advantages of being less toxic and expensive and easily available compared to the noble metals.

This study also shows that molecular copper iodide clusters display very flexible structures, having a great impact on the optical properties. The copper iodide clusters thus appear to be

a general family of mechanochromic compounds. Work in our laboratories is in progress to find other pressure-responsive copper-based systems with even higher sensitivity.

■ ASSOCIATED CONTENT

Supporting Information

The experimental section, the X-ray crystallographic files (CIF), and other characterization data. This material is available free of charge via the Internet at http://pubs.acs.org.

■ AUTHOR INFORMATION

Corresponding Author

sandrine.perruchas@polytechnique.edu

Notes

The authors declare no competing financial interest.

■ ACKNOWLEDGMENTS

The authors thank the CNRS and Ecole Polytechnique for funding. Q.B. thanks the DGA for his Ph.D. fellowship.

■ REFERENCES

(1) Kim, E.; Park, S. B. *Chem.—Asian J.* **2009**, *4*, 1646−1658.
(2) Hirata, S.; Watanabe, T. *Adv. Mater.* **2006**, *18*, 2725−2729.
(3) Beyer, M. K.; Clausen-Schaumann, H. *Chem. Rev.* **2005**, *105*, 2921−2948.
(4) Ariga, K.; Mori, T.; Hill, J. P. *Adv. Mater.* **2012**, *24*, 158−176.
(5) Sagara, Y.; Kato, T. *Nat. Chem.* **2009**, *1*, 605−610.
(6) Ciardelli, F.; Ruggeri, G.; Pucci, A. *Chem. Soc. Rev.* **2013**, *42*, 857−870.
(7) Sage, I.; Bourhill, G. *J. Mater. Chem.* **2001**, *11*, 231−2345.
(8) Balch, A. L. *Angew. Chem., Int. Ed.* **2009**, *48*, 2641−2644 and references therein..
(9) Zhang, X.; Chi, Z.; Zhang, Y.; Liu, S.; Xu, J. *J. Mater. Chem. C* **2013**, *1*, 3376−3396.
(10) Themed issue: "Mechanoresponsive Materials". *J. Mater. Chem.* **2011**, *21* (23).
(11) Roberts, D. R. T.; Holder, S. J. *J. Mater. Chem. C* **2011**, *21*, 8256−8268.
(12) Sagara, Y.; Kato, T. *Angew. Chem., Int. Ed.* **2011**, *50*, 9128−9132.
(13) Nagura, K.; Saito, S.; Yusa, H.; Yamawaki, H.; Fujihisa, H.; Sato, H.; Shimoikeda, Y.; Yamaguchi, S. *J. Am. Chem. Soc.* **2013**, *135*, 10322−10325.
(14) Zhang, X.; Chi, Z.; Zhang, Y.; Liu, S.; Xu, J. *J. Mater. Chem. C* **2013**, *1*, 3376−3390.
(15) Chi, Z.; Zhang, X.; Xu, B.; Zhou, X.; Ma, C.; Zhang, Y.; Liu, S.; Xu, J. *Chem. Soc. Rev.* **2012**, *41*, 3878−3896.
(16) Zn complexes. (a) Mizukami, S.; Houjou, H.; Sugaya, K.; Koyama, E.; Tokuhisa, H.; Sasaki, T.; Kanesato, M. *Chem. Mater.* **2005**, *17*, 50−56. (b) Xu, B.; Chi, Z.; Zhang, X.; Li, H.; Chen, C.; Liu, S.; Zhang, Y.; Xu, J. *Chem. Commun.* **2011**, *47*, 11080−11082. (c) Tzeng, B.-C.; Chang, T.-Y.; Wei, S.-L.; Sheu, H.-S. *Chem.—Eur. J.* **2012**, *18*, 5105−5112.
(17) Ag complexes. (a) Tsukuda, T.; Kawase, M.; Dairiki, A.; Matsumoto, K.; Tsubomura, T. *Chem. Commun.* **2010**, *46*, 1905−1907. (b) Babashkina, M. G.; Safin, D. A.; Bolte, M.; Garcia, Y. *Dalton Trans.* **2011**, *40*, 8523−8526.
(18) Be complex. Cheng, X.; Zhang, H.; Ye, K.; Zhang, H.; Wang, Y. *J. Mater. Chem. C* **2013**, *1*, 7507−7512.
(19) Pd complex. Grey, J. K.; Butler, I. S.; Reber, C. *Inorg. Chem.* **2003**, *42*, 6503−6518.
(20) Al complexes. (a) Bi, H.; Chen, D.; Li, D.; Yuan, Y.; Xia, D.; Zhang, Z.; Zhang, H.; Wang, Y. *Chem. Commun.* **2011**, *47*, 4135−4137. (b) Yan, D.; Lu, J.; Ma, J.; Qin, S.; Wei, M.; Evans, D. G.; Duan, X. *Angew. Chem., Int. Ed.* **2011**, *50*, 7037−7040.
(21) Ir complexes. (a) Mastropietro, T. F.; Yadav, Y. J.; Szerb, E. I.; Talarico, A. M.; Ghedini, M.; Crispini, A. *Dalton Trans.* **2012**, *41*, 8899−8907. (b) Szerb, E. I.; Talarico, A. M.; Aiello, I.; Crispini, A.; Godbert, N.; Pucci, D.; Pugliese, T.; Ghedini, M. *Eur. J. Inorg. Chem.* **2010**, 3270−3277. (c) Shan, G.-G.; Li, H.-B.; Cao, H.-T.; Zhu, D.-X.; Li, P.; Su, Z.-M.; Liao, Y. *Chem. Commun.* **2012**, *48*, 2000−2002. (d) Shan, G.-G.; Li, H.-B.; Qin, J.-S.; Zhu, D.-X.; Liao, Y.; Su, Z.-M. *Dalton Trans.* **2012**, *41*, 9590−9593. (e) Shan, G.-G.; Li, H.-B.; Zhu, D.-X.; Su, Z.-M.; Liao, Y. *J. Mater. Chem. C* **2012**, *22*, 12736−12744.
(22) Au complexes. (a) Ito, H.; Saito, T.; Oshima, N.; Kitamura, N.; Ishizaka, S.; Hinatsu, Y.; Wakeshima, M.; Kato, M.; Tsuge, K.; Sawamura, M. *J. Am. Chem. Soc.* **2008**, *130*, 10044−10045. (b) Lee, Y.-A.; Eisenberg, R. *J. Am. Chem. Soc.* **2003**, *125*, 7778−7779. (c) Schneider, J.; Lee, Y.-A.; Pérez, J.; Brennessel, W. W.; Flaschenriem, C.; Eisenberg, R. *Inorg. Chem.* **2008**, *47*, 957−968. (d) Catalano, V. J.; Horner, S. J. *Inorg. Chem.* **2003**, *42*, 8430−8438. (e) Assefa, Z. A.; Omary, M.; McBurnett, B. G.; Mohamed, A. A.; Patterson, H. H.; Staples, R. J.; Fackler, J. P. *Inorg. Chem.* **2002**, *41*, 6274−6280. (f) Assefa, Z. A.; Omary, M.; McBurnett, B. G.; Mohamed, A. A.; Patterson, H. H.; Staples, R. J.; Fackler, J. P. *Inorg. Chem.* **2002**, *41*, 6274−6280. (g) Laguna, A.; Lasanta, T.; Lopez-de-Luzuriaga, J. M.; Monge, M.; Naumov, P.; Olmos, M. E. *J. Am. Chem. Soc.* **2010**, *132*, 456−457. (h) Osawa, M.; Kawata, I.; Igawa, S.; Hoshino, M.; Fukunaga, T.; Hashizume, D. *Chem.—Eur. J.* **2010**, *16*, 12114−12126. (i) Koshevoy, I. O.; Lin, C.-L.; Karttunen, A. J.; Haukka, M.; Shih, C.-W.; Chou, P.-T.; Tunik, S. P.; Pakkanen, T. A. *Chem. Commun.* **2011**, *47*, 5533−5535. (j) Ito, H.; Muromoto, M.; Kurenuma, S.; Ishizaka, S.; Kitamura, N.; Sato, H.; Seki, T. *Nat. Commun.* **2013**, *4*, 2009−2014.
(23) Pt complexes. (a) Kozhevnikov, V. N.; Donnio, B.; Bruce, D. W. *Angew. Chem., Int. Ed.* **2008**, *47*, 6286. (b) Abe, T.; Itakura, T.; Ikeda, N.; Shinozaki, K. *Dalton Trans.* **2009**, 711−715. (c) Ni, J.; Zhang, X.; Wu, Y.-H.; Zhang, L.-Y.; Chen, Z.-N. *Chem.—Eur. J.* **2011**, *17*, 1171−1183. (d) Nishiuchi, Y.; Takayama, A.; Suzuki, T.; Shinozaki, K. *Eur. J. Inorg. Chem.* **2011**, 1815. (e) Choi, S. J.; Kuwabara, J.; Nishimura, Y.; Arai, T.; Kanbara, T. *Chem. Lett.* **2012**, *41*, 65. (f) Zhang, X.; Wang, J.-Y.; Ni, J.; Zhang, L.-Y.; Chen, Z.-N. *Inorg. Chem.* **2012**, *51*, 5569−5579. (g) Huang, L.-M.; Tu, G.-M.; Chi, Y.; Hung, W.-Y.; Song, Y.-C.; Tseng, M.-R.; Chou, P.-T.; Lee, G.-H.; Wong, K.-T.; Cheng, S.-H.; Tsai, W.-S. *J. Mater. Chem. C* **2013**, *1*, 7582−7592. (h) Ni, J.; Zhang, X.; Qui, N.; Wu, Y.-H.; Zhang, L.-Y.; Zhang, J.; Chen, Z.-N. *Inorg. Chem.* **2011**, *50*, 9090−9096. (i) Huang, L.-M.; Tu, G.-M.; Chi, Y.; Hung, W.-Y.; Song, Y.-C.; Tseng, M.-R.; Chou, P.-T.; Lee, G.-H.; Wong, K.-T.; Cheng, S.-H.; Tsai, W.-S. *J. Mater. Chem. C* **2013**, *1*, 7582−7592.
(24) Perruchas, S.; Le Goff, X. F.; Maron, S.; Maurin, I.; Guillen, F.; Garcia, A.; Gacoin, T.; Boilot, J.-P. *J. Am. Chem. Soc.* **2010**, *132*, 10967−10969.
(25) (a) Wen, T.; Zhang, D.-X.; Liu, J.; Lin, R.; Zhang, J. *Chem. Commun.* **2013**, *49*, 5660−5662. (b) Shan, X.-C.; Jiang, F.-L.; Chen, L.; Wu, M.-Y.; Pan, J.; Wan, X.-Y.; Hong, M.-C. *J. Mater. Chem. C* **2013**, 4339−4349. (c) Shan, X.-C.; Zhang, H.-B.; Chen, L.; Wu, M.-Y.; Jiang, F.-L.; Hong, M.-C. *Cryst. Growth Des.* **2013**, *13*, 1377−1381.
(26) Sagara, Y.; Mutai, T.; Yoshikawa, I.; Araki, K. *J. Am. Chem. Soc.* **2007**, *129*, 1520−1521.
(27) Bernstein, J. *Polymorphism in Molecular Crystals*; Clarendon Press: Oxford, 2002.
(28) Mutai, T.; Satou, H.; Araki, K. *Nat. Mater.* **2005**, *4*, 685−687.
(29) Zhang, H.; Zhang, Z.; Ye, K.; Zhang, J.; Wang, Y. *Adv. Mater.* **2006**, *18*, 2369−2372.
(30) Abe, Y.; Karasawa, S.; Koga, N. *Chem.—Eur. J.* **2012**, *18*, 15038−15048.
(31) Gu, X.; Yao, J.; Zhang, G.; Zhang, D. *Small* **2012**, *22* (8), 3406−3411.
(32) Chang, Y. C.; Wang, S. L. *J. Am. Chem. Soc.* **2012**, *134*, 9848−9851.
(33) Brinkmann, M.; Gadret, G.; Muccini, M.; Taliani, C.; Masciocchi, N.; Sironi, A. *J. Am. Chem. Soc.* **2000**, *122*, 5147−5157.
(34) (a) Malwitz, M. A.; Lim, S. H.; White-Morris, R. L.; Pham, D. M.; Olmstead, M. M.; Balch, A. L. *J. Am. Chem. Soc.* **2012**, *134*, 10885−10893. (b) Manbeck, G. F.; Brennessel, W. W.; Stockland, R.

A.; Eisenberg, R. *J. Am. Chem. Soc.* **2010**, *132*, 12307−12318. (c) Koshevoy, I. O.; Chang, Y.-C.; Karttunen, A. J.; Haukka, M.; Pakkanen, T.; Chou, P.-T. *J. Am. Chem. Soc.* **2012**, *134*, 6564−6567.
(35) (a) Komiya, N.; Itami, N.; Naota, T. *Chem.—Eur. J.* **2013**, *19*, 9497−9505. (b) Diez, A.; Fornies, J.; Larraz, C.; Lalinde, E.; Lopez, J. A.; Martin, A.; Moreno, M. T.; Sicilia, V. *Inorg. Chem.* **2010**, *49*, 3239−3251.
(36) (a) Zhang, G.; Lu, J.; Sabat, M.; Fraser, C. L. *J. Am. Chem. Soc.* **2010**, *132*, 2160−2162. (b) Dong, Y.; Xu, B.; Zhang, J.; Tan, X.; Wang, L.; Chen, J.; Lv, H.; Wen, S.; Li, B.; Ye, L.; Zou, B.; Tian, W. *Angew. Chem., Int. Ed.* **2012**, *51*, 10782−10785. (c) Gu, X.; Yao, J.; Zhang, G.; Yan, Y.; Zhang, C.; Peng, Q.; Liao, Q.; Wu, Y.; Xu, Z.; Zhao, Y.; Fu, H.; Zhang, D. *Adv. Funct. Mater.* **2012**, *22*, 4862−4872. (d) Yoon, S.-J.; Park, S. Y. *J. Mater. Chem.* **2011**, *21*, 8338−8346. (e) Zhao, N. *Chem. Commun.* **2012**, *48*, 8637−8639. (f) Chang, Y.-C.; Wang, S.-L. *J. Am. Chem. Soc.* **2012**, *134*, 9848−9851. (g) Yoon, S.-J.; Park, S. Y. *J. Mater. Chem.* **2011**, *21*, 8338−8346. (h) Qi, Q.; Zhang, J.; Xu, B.; Li, B.; Zhang, S. X.-A.; Tian, W. *J. Phys. Chem. C* **2013**, *117*, 24997−25003.
(37) Tard, C.; Perruchas, S.; Maron, S.; Le Goff, X. F.; Guillen, F.; Garcia, A.; Vigneron, J.; Etcheberry, A.; Gacoin, T.; Boilot, J.-P. *Chem. Mater.* **2008**, *20*, 7010−7016.
(38) Perruchas, S.; Desboeufs, N.; Maron, S.; Le Goff, X. F.; Fargues, A.; Garcia, A.; Gacoin, T.; Boilot, J.-P. *Inorg. Chem.* **2012**, *51*, 794−798.
(39) Bondi, A. *J. Phys. Chem.* **1964**, *68*, 441.
(40) Olivieri, A. *J. Am. Chem. Soc.* **1992**, *114*, 5758.
(41) Harris, R. K.; Olivieri, A. *Prog. Nucl. Magn. Reson. Spectrosc.* **1992**, *24*, 435.
(42) Sokolov, F. D.; Babashkina, M. G.; Fayon, F.; Rakhmatullin, A. I.; Safin, D. A.; Pape, T.; Hahn, F. E. *J. Organomet. Chem.* **2009**, *694*, 167.
(43) Tang, J. A.; Ellis, B. D.; Warren, T. H.; Hanna, J. D.; Macdonald, C. L. B.; Schurko, R. W. *J. Am. Chem. Soc.* **2007**, *129*, 13049.
(44) Rusanovam, D.; Forsling, W.; Antzutkin, O. N.; Pike, K. J.; Dupree, R. J. *Magn. Reson* **2006**, *179*, 140.
(45) Rusanovam, D.; Forsling, W.; Antzutkin, O. N.; Pike, K. J.; Dupree, R. *Langmuir* **2005**, *21*, 4420.
(46) Rusanovam, D.; Pike, K. J.; Persson, I.; Dupree, R.; Lindberg, M.; Hanna, J. V.; Antzutkin, O. N.; Forsling, W. *Polyhedron* **2006**, *25*, 3569.
(47) O'Dell, L. A.; Rossini, A. J.; Schurko, R. W. *Chem. Phys. Lett.* **2009**, *468*, 330.
(48) Perruchas, S.; Tard, C.; Le Goff, X. F.; Fargues, A.; Garcia, A.; Kahlal, S.; Saillard, J.-Y.; Gacoin, T.; Boilot, J.-P. *Inorg. Chem.* **2011**, *50*, 10682−10692.
(49) Hardt, H. D.; Pierre, A. Z. *Anorg. Allg. Chem.* **1973**, *402*, 107.
(50) Ford, P. C.; Cariati, E.; Bourasssa, J. *Chem. Rev.* **1999**, *99*, 3625−3647.
(51) Kyle, K. R.; Ryu, C. K.; DiBenedetto, J. A.; Ford, P. C. *J. Am. Chem. Soc.* **1991**, *113*, 2954.
(52) Kim, T. H.; Shin, Y. W.; Jung, J. H.; Kim, J. S.; Kim, J. *Angew. Chem., Int. Ed.* **2008**, *47*, 685−688.
(53) Kitagawa, H.; Ozawa, Y.; Toriumi, K. *Chem. Commun.* **2010**, *46*, 6302−6304.